

CONTENTS

Abstract (in Chinese).....	i
Abstract (in English)	ii
Acknowledgement.....	iii
Contents	iv
List of table	vi
List of figures.....	vii

Chapter 1 : Introduction 1

1.1 Narrow linewidth source for fiber lasers	1
1.1.1. The development of versatile fiber lasers sources	1
1.1.2. Mutual injection locking and mode beating noise...	2
1.1.3. Motivations for generating narrow linewidth and mode beating noise-free source.....	3
1.2 All-Optical Data Processing by Using Injection-Locked Lasers...4	4
1.2.1. Versatile NRZ-to-PRZ transformer by using FPLD	4
1.2.2. Motivations for generating a simple NRZ-to-RZ data transformer	5
1.3 The introduction of chapters.....	5

Chapter 2 : Theory and Experiments of a Mode Beating Noise Suppressed and Mutually Injection-Locked Fabry-Perot Laser Diode and Erbium-Doped Fiber Amplifier Link 7

2.1 Abstract	7
2.2 Introduction.....	7
2.3 Experimental Setup	9
2.4 Theoretical Simulation of SMSR and Linewidth.....	12
2.5 Laser Linewidth Measurement	20
2.5.1. Heterodyne Using a Local Oscillator.....	20
2.5.2. Delayed Self-Homodyne	23
2.6 Results and Discussion.....	25
2.6.1. Free-running FPLD and EDL	25
2.6.2. EDL-FPLD Link with Close-loop EDFA	27
2.6.3. EDFA-FPLD Link with Open-loop EDFA.....	29
2.6.4. Discussion	32

2.7 Conclusion	34
Chapter 3 : All-optical NRZ-to-PRZ format transformer by injection-locking an Fabry-Perot laser diode at unlasing condition.....	36
3.1 Abstract	36
3.2 Introduction	37
3.3 Experimental setup and Principle of Operation	39
3.4 Results and discussion.....	44
3.4.1. CW external injection.....	44
3.4.2. External injection by PRBS coding	49
3.5 Applications	57
3.6 Conclusion	59
Chapter 4 : Summary.....	61
References.....	63
Publication list	67



LIST OF TABLE

Table 2.1	The 3-dB linewidths ($\Delta\lambda$), SMSR, and required injecting power for the FPLD at different laser configurations.....	32
Table 3.1	Comparison among versatile NRZ-to-PRZ techniques.....	57
Table 3.2	Truth table for all-optical OR operation.	59



LIST OF FIGURES

Fig. 2.1	The block diagrams of experimental setup. (a) the free-running EDL without or with the OBPF (b) the configuration for an EDL-FPLD link (c) the configuration for an EDFA-FPLD link	12
Fig. 2.2	The mutually injection seeding scheme between FPLD and filtered EDL (or EDFA).....	14
Fig. 2.3	The theoretically simulated SMSR of the mutually injection-locked EDL-FPLD as function of reflectivity change (ΔR) and the ratio of loss coefficient (Γ_1/Γ_2).....	17
Fig. 2.4	The change of loss coefficient ($\Delta\Gamma$) as a function of reflectivity change (ΔR) under the mutual injection-locking condition.....	18
Fig. 2.5	The simulated linewidth of mutually injection-locked EDL-FPLD link as a function of reflectivity change (ΔR).....	19
Fig. 2.6	Optical heterodyne setup for measuring laser linewidth using an external cavity laser for local oscillator.....	20
Fig. 2.7	The mixing process in terms of beat-tone slices mixed down to low frequencies that can be analyzed with electronic instrumentation.....	21
Fig. 2.8	Convolution of narrow linewidth laser translates signal spectrum to low frequencies.....	23
Fig. 2.9	Optical delayed self-homodyne measurement set-up for laser linewidth measurement.....	24
Fig. 2.10	The delayed self-homodyne mixing of the laser filed with itself.....	25

Fig. 2.11	The lasing and mode-beating spectra of a commercial DFBLD (a) and (b), a CW lasing FPLD (c) and (d), and a free-running EDFL (e) and (f), respectively.	27
Fig. 2.12	The lasing spectra of an mutually injection-locked EDFL-FPLD link with the FPLD at different biased currents.	28
Fig. 2.13	The comparison on the mode-beating spectra of DFBLD, mutually injection-locked EDFL-FPLD link, and EDFA-FPLD link.	29
Fig. 2.14	The optical spectra of mutually injection-locked EDFA-FPLD link with different coupling schemes (a) 5% EDFA feedback injects into the FPLD (b) 95% EDFA feedback injects into the FPLD (c) 50% EDFA feedback injects into the FPLD.	30
Fig. 2.15	The lasing spectra of (I) free-running EDFL, (II) OBPF filtered EDFL, (III) mutually injection-locked EDFL-FPLD link, and (IV) mutually injection-locked EDFA-FPLD link.	31
Fig. 2.16	The lasing and mode-beating spectra of EDFL-FPLD (a) and (b), and EDFA-FPLD links (c) and (d).	33
Fig. 2.17	The output power and gain characteristics of EDFA at different input powers.	34
Fig. 3.1	Experimental setup for the NRZ-to-PRZ format transformer.....	40
Fig. 3.2	The characteristic transmission coefficient of MZM at different DC bias.....	41
Fig. 3.3	(a) The ‘general’ gain-switching method; (b) The ‘anomalous’ gain-switching method: (A) without external injection; (B) with external injection	42
Fig. 3.4	The evolution of pulse-shape under the external injection at different wavelengths.....	44
Fig. 3.5	The OOK pulse shape of the injection-locked FPLD at “on”	

and “off” states with repetition rate of 1 GHz.....	45
Fig. 3.6 The linewidth comparison of the CW free-running FPLD, the CW tunable laser, and the gain-switched FPLD.....	46
Fig. 3.7 The extinction ratio of the injection-locked FPLD at different RF and external injection power.....	47
Fig. 3.8 The peak power and the SMSR of the single-mode gain-switched FPLD at OOK mode	47
Fig. 3.9 The SSB phase noise density and associated timing jitter of the injection-locked FPLD pulses.....	48
Fig. 3.10 Timing jitter and pulselwidth versus external injection power.....	49
Fig. 3.11 RZ data stream (a) without OBPF (b) with OBPF	49
Fig. 3.12 The patterns: (a) the electrical NRZ data before the MZM; (b) the PG-encoded external injection light; (c) the transformed PRZ signal generated from the injection-locked FPLD	50
Fig. 3.13 The corresponding eye diagrams: (a) the electrical NRZ data before the MZM; (b) the PG-encoded external injection light; (c) the transformed PRZ signal generated from the single-mode FPLD. The data rate is 2.488 Gbit/s	51
Fig. 3.14 The BER against the received optical power for NRZ-encoded external injection light and transformed PRZ signal at data rate of 2.488 Gbit/s	52
Fig. 3.15 The BERs for different external injection powers at data rate of 2.488 Gbit/s.....	52
Fig. 3.16 The variation of OOK data rate at different FPLD’s DC bias	53
Fig. 3.17 The patterns: (a) the electrical NRZ data before the MZM; (b) the PG-encoded external injection light; (c) the transformed	

PRZ signal generated from the injection-locked FPLD. The data rate is 9.953 Gbit/s	54
--	----

Fig. 3.18 The corresponding eye diagrams: (a) the electrical NRZ data before the MZM; (b) the PG-encoded external injection light; (c) the transformed PRZ signal generated from the single-mode FPLD. The data rate is 9.953 Gbit/s	55
--	----

Fig. 3.19 The BER against the received optical power for NRZ-encoded external injection light and transformed PRZ signal at data rate of 9.953 Gbit/s	56
---	----

Fig. 3.20 The BERs for different external injection powers at data rate of 9.953 Gbit/s.....	56
--	----

Fig. 3.21 An all-optical logical OR gate by using the NRZ-to-PRZ format transformer.....	57
--	----

Fig. 3.22 Illustration of the input data (Ch1 and Ch2) and the transformed PRZ signal at data rate of 2.488 GHz.	58
---	----

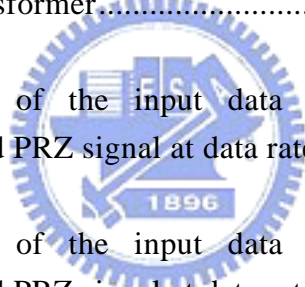


Fig. 3.23 Illustration of the input data (Ch1 and Ch2) and the transformed PRZ signal at data rate of 9.953 GHz	59
---	----